AUTHOR'S PERSONAL COPY

CONFIDENTIAL

Copy RM L52K21

Paul G. Pournier

NACA

RESEARCH MEMORANDUM

EFFECT OF LEADING-EDGE CHORD-EXTENSIONS ON SUBSONIC

AND TRANSONIC AERODYNAMIC CHARACTERISTICS

OF THREE MODELS HAVING 45° SWEPTBACK

WINGS OF ASPECT RATIO 4

By Kenneth W. Goodson and Albert G. Few, Jr.

Langley Aeronautical Laboratory Langley Field, Va.

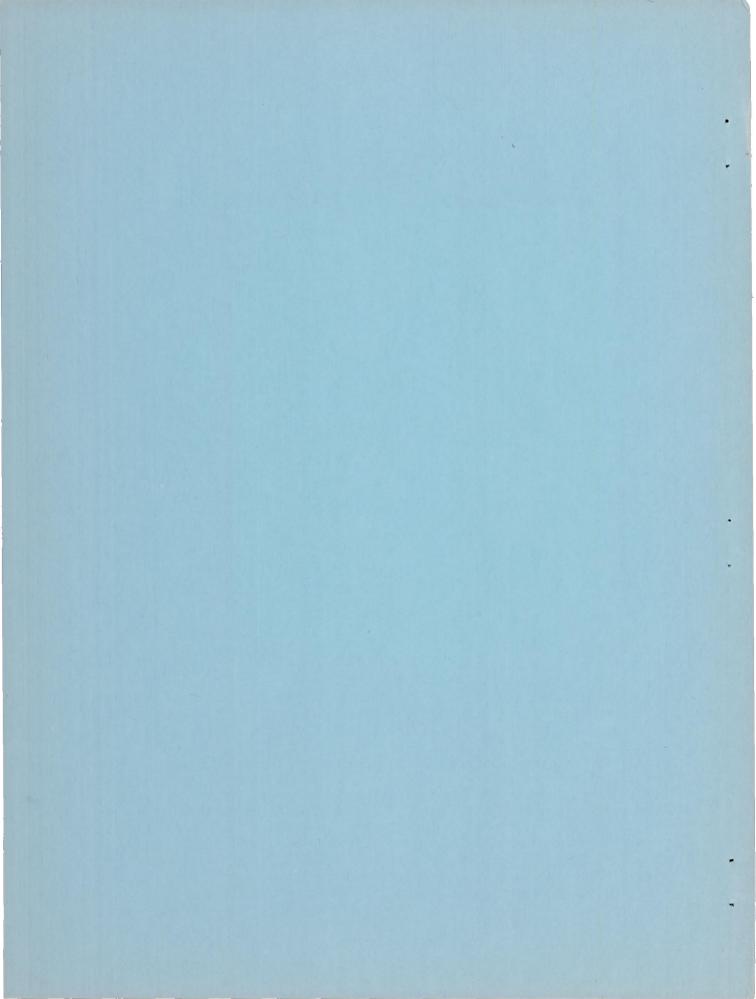
CLASSIFIED DOCUMENT

This material contains information affecting the National Defense of the United States within the meaning of the espionage laws, Title 18, U.S.C., Secs. 793 and 794, the transmission or revelation of which in any manner to an unauthorized person is prohibited by law.

NATIONAL ADVISORY COMMITTEE FOR AERONAUTICS

WASHINGTON

January 21, 1953



NATIONAL ADVISORY COMMITTEE FOR AERONAUTICS

RESEARCH MEMORANDUM

EFFECT OF LEADING-EDGE CHORD-EXTENSIONS ON SUBSONIC

AND TRANSONIC AERODYNAMIC CHARACTERISTICS

OF THREE MODELS HAVING 45° SWEPTBACK

WINGS OF ASPECT RATIO 4

By Kenneth W. Goodson and Albert G. Few, Jr.

SUMMARY

An investigation has been made to determine the effect of leadingedge chord-extensions on high-lift pitching moment and on performance characteristics at subsonic and transonic speeds. Three models were used, each having wings of identical geometry: 45° sweepback, aspect ratio 4, taper ratio 0.3, and NACA 65A006 airfoil sections. The optimum inboard-end location of the chord-extension (0.65b/2) from considerations of low-speed high-lift longitudinal stability characteristics was selected from a study of a wing-alone model in the Langley 300 MPH 7- by 10-foot tunnel. This optimum configuration was incorporated into a wingfuselage model and investigated in the Langley high speed 7- by 10-foot tunnel to Mach numbers of the order of 0.93. This investigation indicated that the longitudinal stability characteristics of the model showed improvements which decreased as a Mach number of 0.90 was approached. In addition, some data were obtained at high subsonic Mach numbers with a full-chord fence mounted at the same spanwise position as the inboard end of the optimum chord-extension. This fence was less effective than the chord-extension. The chord-extension increased the minimum drag very slightly at Mach numbers above 0.80, but generally improved the drag characteristics at high lift coefficients. Data also were obtained through a Mach number range of approximately 0.6 to 1.10 by the use of a small semispan model. The results of this investigation agreed qualitatively with the larger wing-fuselage-model results in regard to beneficial effects of chord-extensions on the pitching-moment characteristics below a Mach number of 0.93. Moreover, with the exception of a Mach number of 0.95, the small semispan-model results indicated benefits up to the highest test Mach number (1.10). Increasing the overhang of the chord-extension from 10 to 15 percent of the mean aerodynamic chord resulted in further improvement in the higher-lift pitching-moment characteristics at all Mach numbers investigated but also caused a larger forward shift in aerodynamic center at low lift coefficients.

TNTRODUCTION

Many current airplane designs having thin sweptback wings have exhibited undesirable stability characteristics in the high-lift range as a result of flow separation over the wing tips. Flow surveys have shown that tip separation is strongly influenced by a leading-edge separation vortex being generated on the upper surface of the wing. (See refs. 1, 2, and 3 for more details on this type of flow phenomena.) Low-speed wind-tunnel tests (refs. 3 and 4) have shown that the high-lift stability characteristics could be improved by causing the leading-edge separation vortex to shed from the wing before growing large enough to cause tip separation. This controlled shedding of the leading-edge vortex can be effected by use of a physical barrier such as a fence or by a chordwise discontinuity such as a chord-extension, which seems to provide an aerodynamic barrier to the growth of the leading-edge vortex.

Although low-speed results of several investigations of chordextensions are available, little information exists pertaining to the effects of chord-extensions on high-subsonic and transonic aerodynamic characteristics. The purpose of the present investigation, therefore, was to determine to what extent the gains realized through the use of chord-extensions at low speed are retained throughout the subsonic and transonic speed range. In this investigation it was found expedient to use three models of identical wing geometry; that is, 45° sweepback, aspect ratio 4, taper ratio 0.3, and NACA 65A006 airfoil sections. The optimum low-speed inboard-end location of the chord-extension was developed from a study of a wing-alone model in the Langley 300 MPH 7- by 10-foot tunnel. This optimum configuration was incorporated into a wing-fuselage model and investigated in the Langley high-speed 7- by 10-foot tunnel to Mach numbers of the order of 0.93. The high-speed results were further extended to a Mach number of 1.10 by use of a small semispan wing model. In addition, some comparative data were obtained at high subsonic speeds with a full-chord fence fixed on the wing-fuselage model at the same location as that used for the inboard end of the leading-edge chord-extension. A partial summary of the present investigation is included in reference 5.

SYMBOLS

 $\mathtt{C}_{\mathtt{L}}$ lift coefficient, $\frac{\mathtt{Lift}}{\mathtt{qS}}$

C_D drag coefficient, Drag

C_{m}	pitching-moment coefficient referred to 0.25c,
	Pitching moment
	qSē
c_{B}	root bending-moment coefficient due to lift, $\frac{\text{Bending moment}}{q \frac{S}{2} \frac{b}{2}}$
$(L/D)_{\max}$	maximum lift-drag ratio
S	wing area based on wing area without chord-extensions, sq ft
ē	mean aerodynamic chord of wing, $\frac{2}{s} \int_0^{b/2} e^{2} dy$, ft
С	local wing chord, parallel to plane of symmetry, ft
Ъ	wing span, ft
У	spanwise distance from plane of symmetry, ft
yc.p.	lateral center of pressure, percent semispan, 100 $\frac{C_B}{C_T}$,
	where C_{B} is measured from C_{L} = 0
q.	effective dynamic pressure, $\frac{\rho V^2}{2}$, lb/sq ft
ρ	air density, slugs/cu ft
V	stream velocity over span of model, ft/sec
М	effective Mach number over span of model
MZ	local Mach number
Ma	average chordwise Mach number
R	mean test Reynolds number of wing based on \bar{c}
α	angle of attack of fuselage center line and wing chord line, deg

in table I.

MODELS AND APPARATUS

The wings tested had 45° sweepback referred to the quarter-chord line, an aspect ratio 4, taper ratio 0.3, and NACA 65A006 airfoil sections parallel to the free stream.

A wing-alone configuration, tested in the Langley 300 MPH 7- by 10-foot tunnel on a single-strut support, incorporated chord-extensions having $0.10\overline{c}$ overhang and various inboard-end locations. (See fig. 1.) The chord-extensions were fabricated in such a manner as to maintain the original contour of the wing-nose section. One chord-extension, having a $0.10\overline{c}$ overhang at its inboard-end (0.65b/2 position) and tapering to zero overhang at the tip, also was tested. (See fig. 1(a).)

The chord-extension having an optimum inboard-end location of 65-percent wing semispan (as determined from a consideration of low-speed longitudinal stability characteristics) and a 0.10c overhang was incorporated on a wing-fuselage model and was tested on the sting support in the Langley high-speed 7- by 10-foot tunnel (fig. 2). The chord-extension of this model was made by cutting the wing along the 0.20c line and using an insert to extend the nose section forward 0.10c. The two segments of the airfoil (nose and trailing-edge sections) were faired

as shown by figure 2(a). A $\frac{1}{16}$ - inch-thick dural fence (fig. 2(a)), located at the 65-percent semispan position of the wing, was also tested on the wing-fuselage model. Fuselage ordinates for the model are given

In order to extend the investigation to higher transonic speeds, a small semispan wing-alone model (fig. 3) was fitted with 0.10\overline{c} and 0.15\overline{c} chord-extensions (inboard end located at the 65-percent semispan position) and was tested in the presence of a reflection-plane plate in the Langley high-speed 7- by 10-foot tunnel. It should be pointed out that the reflection-plane model had previously been used in several investigations in which parts of the model were physically altered and that this model was restored as closely as possible to its original condition. The chord-extensions of the semispan model were fabricated by soldering a sheet-metal "glove" over the wing leading edge in such a manner as to maintain the thickness distribution of the original nose section. The glove was faired tangent to the original airfoil section as shown in figure 3(a).

TESTS

Wing-Alone Model

The wing-alone model was tested on the single-strut support in the Langley 300 MPH 7- by 10-foot tunnel at a Mach number of about 0.17, which corresponds to a Reynolds number of about 1.62×10^6 based on the mean aerodynamic chord of the wing for average test conditions. Tests were made through an angle-of-attack range from about -4° to 30° .

Wing-Fuselage Model

The sting-supported wing-fuselage model was tested in the Langley high-speed 7- by 10-foot tunnel through a Mach number range of approximately 0.40 to 0.93 and through an angle-of-attack range of about -2° to 24° . The variation of Reynolds number through the Mach number range is shown in figure 4.

Semispan Model

The small semispan model was tested in the Langley high-speed 7- by 10-foot tunnel through a Mach number range of approximately 0.60 to 1.10. The model was mounted on a reflection-plane plate (fig. 3(a)) located 3 inches from the tunnel wall in order to by-pass the tunnel-wall boundary layer. At the higher tunnel air speeds, the presence of the reflection-plane plate created a high-local-velocity field which allowed testing the small model up to a Mach number of about 1.10 before choking occurred in the tunnel. The effective test Mach numbers in the longitudinal plane were obtained from contour charts similar to those shown in figure 5 by the use of the relationship

$$M = \frac{2}{S} \int_{0}^{b/2} cM_a dy$$

Gradients in the vertical plane were found to be small. For a more detailed description of the test techniques used in conjunction with the reflection-plane model, see reference 6.

CORRECTIONS

With the exception of a fuselage base-pressure correction to the drag of the wing-fuselage model, no corrections for model-support tares have been applied to the present results. For the wing-fuselage model, the corrected drag data are applicable to a condition of free-stream static pressure at the fuselage base. From past experience, it is expected that the influence of the sting support used with the wing-fuselage model is negligible with regard to lift and pitching moments. The single vertical support used with the wing-alone model may have had significant tare effects; however, such effects should not alter the comparative value of results obtained with the various modifications. It is assumed that no tare effects existed in the case of the small semispan model. The data obtained from all three model setups have been corrected for tunnel air-flow misalinement.

Wing-Alone Model

In order to account for flow-constriction effects with the wingalone model in the tunnel, blockage corrections were applied by the method of reference 7. The angle of attack and the drag data of this model were corrected for jet-boundary effects by the method of reference 8. The jet-boundary correction to the pitching moment was considered negligible and therefore was not applied. Corrections for vertical buoyancy on the support strut and for longitudinal pressure gradient have been applied.

Wing-Fuselage Model

Blockage corrections were applied to the sting-supported wing-fuselage model results by the method of reference 7. Corrections for jet-boundary effects to the angle of attack and drag were applied in accordance with reference 8. The jet-boundary corrections to the pitching moment were considered negligible and therefore were not applied.

Semispan Model

Blockage and jet-boundary corrections to the semispan-model data have not been evaluated because the boundary conditions to be satisfied are not rigorously defined. However, inasmuch as the effective flow field is quite large compared to the model size, these corrections are believed to be small.

RESULTS AND DISCUSSION

Presentation of Results

The results of the low-speed tests to select the optimum inboardend location on the wing-alone model are presented in figure 6. Data obtained throughout the subsonic speed range on the wing-fuselage model are presented in figure 7, and the results of the small-semispan-model investigation at transonic speeds are given in figure 8. Figure 9 presents a summary of some of the aerodynamic parameters obtained from the various models.

As already pointed out the small semispan model had previously been used in several investigations in which parts of the model were physically altered. In order to obtain some insight on the effects of chord extension at higher transonic speeds, this model was restored as closely as possible to its original condition. Because of the low Reynolds number, possible residual asymmetry associated with the restoration of the model, and possible inaccuracies of installing the small chord-extensions, the data obtained are considered to be of questionable quantitative value, although the data should be valid for qualitative interpretation.

Low-Speed Development

The results of the low-speed tests of the basic wing-alone configuration (fig. 6) indicate a pronounced unstable tendency at lift coefficients greater than 0.5. All leading-edge extensions investigated improved the high-lift pitching-moment characteristics. However, of the extensions investigated, an inboard-end location of 0.65b/2 appeared about optimum in that it provided a fairly linear variation of $C_{\rm m}$ with α or with $C_{\rm L}$ to the stall, with about neutral stability at the stall. The improvement in the flow over the outboard wing sections with chord-extensions installed is further shown by an increase in lift at the higher angles of attack. The pitching moments noted at zero angle of attack are believed to be caused by model-support tares; however, such effects should not alter the comparative value of results obtained for the various configurations.

The effect of chord-extension plan form is shown in figure 6(b). From the results, it appears that the tapered extension (having the same inboard-end dimension as the optimum constant chord-extension but tapering to zero overhang at the tip) retained most of the gains of the extension with constant overhang. This result might be expected inasmuch as other investigations (for example, ref. 4) have indicated that the inboard-end location of the chord extension largely determines its effectiveness.

High-Speed Characteristics

Pitching moment.- The basic wing-fuselage model showed unstable tendencies at lift coefficients above 0.5 throughout most of the subsonic speed range (fig. 7) similar to that shown at low speeds for the wing-alone model. Utilization of the chord-extension that was selected from the low-speed investigation delayed the instability to considerably higher lift coefficients and angles of attack, although the departure from linearity is still far from desirable. At Mach numbers near 0.9, it appears that the gains due to the chord-extension are quite small. The effects of replacing the chord-extension with a full-chord fence located at the 65-percent semispan position were also determined for several Mach numbers, and it is apparent that the fence generally is somewhat less effective. Chord-extensions (0.10c) or fences had essentially no effect on the stability characteristics at lift coefficients below 0.4 as shown by the wing-fuselage results. (See fig. 7.)

The results of a transonic investigation on the small semispan model having the same plan form as the wing-fuselage model are presented in figure 8. The small model data with a $0.10\bar{c}$ chord-extension are in qualitative agreement with the wing-fuselage results at Mach numbers below 0.9 and, except for M=0.95, indicate improved pitching-moment characteristics up to the highest Mach number (M=1.10). Increasing the overhang of the chord-extension from $0.10\bar{c}$ to $0.15\bar{c}$ resulted in further improvements in high-lift pitching-moment characteristics at all Mach numbers, particularly at the higher speeds. Increasing the chord-extension overhang also moved the aerodynamic center forward, and this movement became progressively smaller with increase in Mach number. (See fig. 8.)

<u>Lift characteristics.</u> At the higher angles of attack, the increases in lift coefficient of the wing-fuselage model attributable to the extension are somewhat greater (fig. 7) than would be expected from consideration of the 4-percent increase in wing area. The fence produced very little effect on the lift characteristics. The effect of chord-extensions on the lift-curve slopes is shown in figure 9.

Through most of the subsonic speed range, the data obtained with the small semispan model indicate that the lift coefficients at a given angle of attack are increased approximately in proportion to the area ratios in the high-lift range. At Mach numbers above M=0.95, however, the gains in lift coefficient are slightly greater than indicated by the area ratios. Although the small semispan model bending-moment data (fig. 8) are rather scattered, it appears that the center of lift is somewhat farther outboard (as shown by the lateral center-of-pressure data (fig. 9)) for the wing with chord-extensions installed than for the basic wing, particularly at the higher lift coefficients. This indicates that a considerable portion of the gains in longitudinal stability

previously discussed are traceable to a larger proportion of the total load being carried by the wing tips. It should be further noted from the bending-moment data that the structural design loads at the wing root would be increased by the use of chord-extensions.

Drag characteristics.— The results presented in figure 9 indicate that addition of the chord-extension generally increased slightly the drag at zero lift for the wing-fuselage model, particularly at high Mach numbers. This increase is primarily responsible for the 20-percent decrease in the maximum lift-drag ratio at M=0.93. The limited wing-fuselage fence data indicate a performance reduction similar to that obtained with the chord-extension at a Mach number of 0.9. At the higher lift coefficients, the chord-extension improved the drag characteristics for all models.

CONCLUDING REMARKS

An investigation has been made to determine the effects of leading-edge chord-extensions on high-lift stability characteristics and on performance characteristics at subsonic and transonic speeds of models having wings with 45° sweepback and aspect ratio 4. From tests of a wing-fuselage model at high subsonic speeds, it was found that the optimum chord-extension configuration (65-percent semispan inboard-end location) developed from a preliminary low-speed study produced gains in longitudinal stability at the higher lift coefficients that diminished with increasing Mach number. At a Mach number of 0.90, the improvements were quite small. A full-chord fence located at the same spanwise location as the inboard end of the optimum chord-extension was less effective in improving the stability than was the chord-extension. The chord-extension increased slightly the minimum drag at Mach numbers above 0.80 but generally improved the drag characteristics at high lift coefficients.

The results of a transonic investigation of a small-scale semispan model having the same plan form as that of the wing-fuselage model were in qualitative agreement with the large model results in regard to beneficial effects of chord-extensions on the pitching-moment characteristics below a Mach number of 0.93. Moreover, with the exception of the data for a Mach number of 0.95, the small-semispan-model results indicated gains up to the highest Mach number (1.10) attained. Increasing the overhang of the chord extension from 10 to 15 percent of the mean-aerodynamic chord resulted in further improvement in the high-lift

pitching-moment characteristics at all Mach numbers investigated, but also caused a larger forward shift in aerodynamic center at low lift coefficients.

Langley Aeronautical Laboratory,
National Advisory Committee for Aeronautics,
Langley Field, Va.

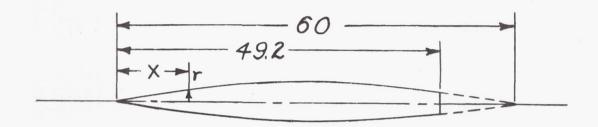
REFERENCES

- 1. Lowry, John G., and Schneiter, Leslie E.: Investigation at Low Speed of the Longitudinal Stability Characteristics of a 60° Swept-Back Tapered Low-Drag Wing. NACA TN 1284, 1947.
- 2. Furlong, G. Chester, and McHugh, James G.: A Summary and Analysis of the Low-Speed Longitudinal Characteristics of Swept Wings at High Reynolds Numbers. NACA RM L52D16, 1952.
- 3. Jaquet, Byron M.: Effects of Chord Discontinuities and Chordwise Fences on Low-Speed Static Longitudinal Stability of an Airplane Model Having a 35° Sweptback Wing. NACA RM L52C25, 1952.
- 4. Goodson, Kenneth W., and Few, Albert G., Jr.: Low-Speed Static Longitudinal and Lateral Stability Characteristics of a Model With Leading-Edge Chord-Extensions Incorporated on a 40° Sweptback Circular-Arc Wing of Aspect Ratio 4 and Taper Ratio 0.50. NACA RM L52I18, 1952.
- 5. Donlan, Charles J., and Weil, Joseph: Characteristics of Swept Wings at High Speeds. NACA RM L52Al5, 1952.
- 6. Spreemann, Kenneth P., and Alford, William J., Jr.: Small-Scale Investigation at Transonic Speeds of the Effects of Thickening the Inboard Section of a 45° Sweptback Wing of Aspect Ratio 4, Taper Ratio 0.3, and NACA 65A006 Airfoil Section. NACA RM L51F08a, 1951.
- 7. Herriot, John G.: Blockage Corrections for Three-Dimensional-Flow Closed-Throat Wind Tunnels, With Consideration of the Effect of Compressibility. NACA Rep. 995, 1950. (Supersedes NACA RM A7B28.)
- 8. Gillis, Clarence L., Polhamus, Edward C., and Gray, Joseph L., Jr.: Charts for Determining Jet-Boundary Corrections for Complete Models in 7- by 10-Foot Closed Rectangular Wind Tunnels. NACA ARR L5G31, 1945.

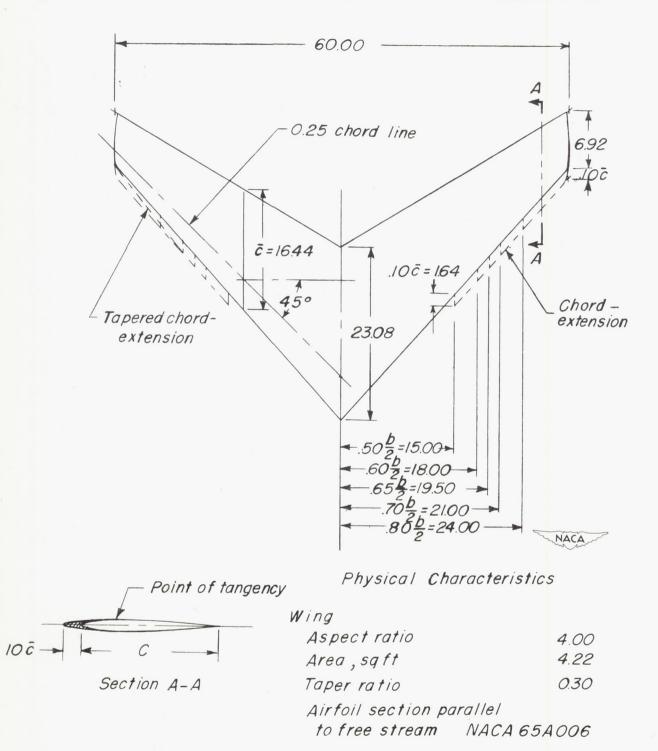
TABLE I

FUSELAGE ORDINATES

[Basic fineness ratio 12; actual fineness ratio 9.8 achieved by cutting off rear portion of body]

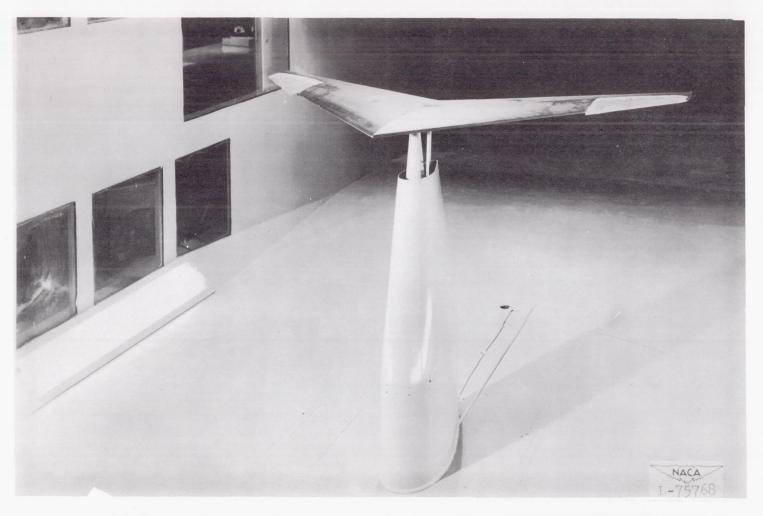


Ordinates,		
x	r	
0 .30 .45 .75 1.50 3.00 4.50 6.00 9.00 12.00 15.00 18.00 21.00 21.00 21.00 33.00 36.00 39.00 49.20	0 •139 •179 •257 •433 •723 •968 1•183 1•556 1•854 2•079 2•245 2•360 2•438 2•438 2•486 2•500 2•478 2•414 2•305 2•137 1•650	
L.E. radius = 0.030		

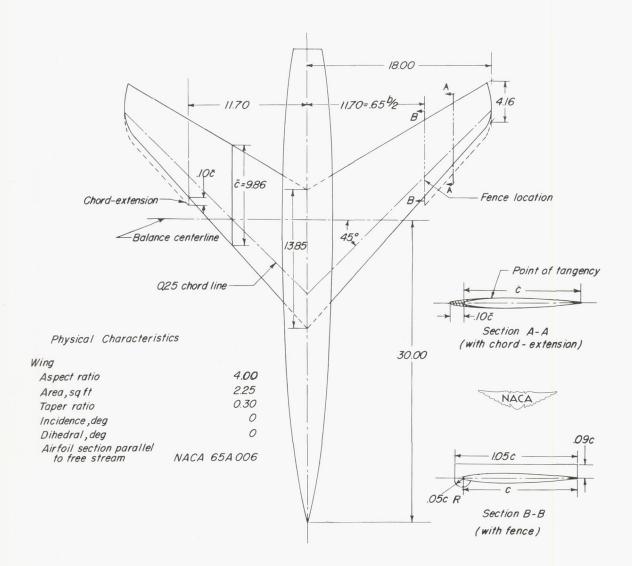


(a) Geometric characteristics of test model. All dimensions are in inches.

Figure 1.- Wing-alone configuration.

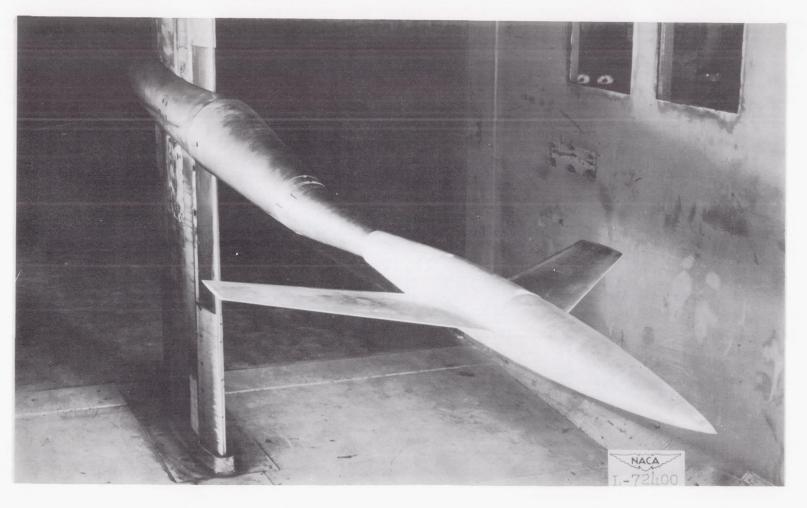


(b) Test model mounted on single support in the Langley 300 MPH 7- by 10-foot tunnel.



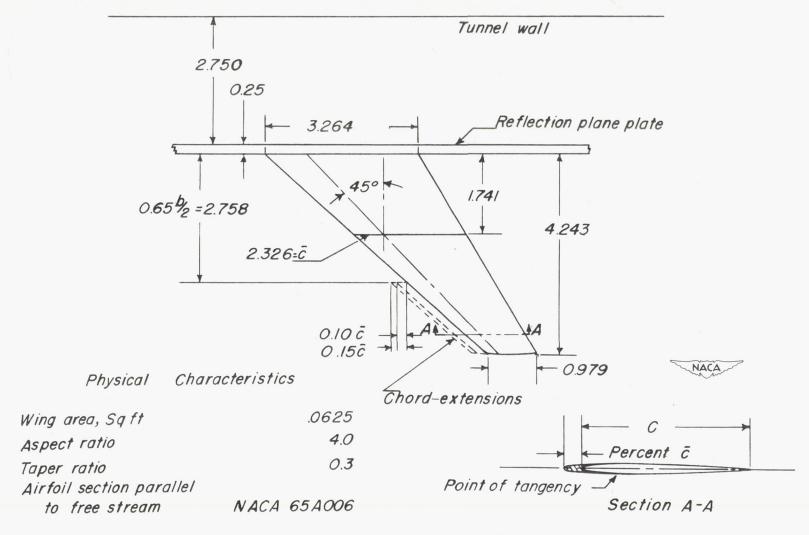
(a) Geometric characteristics of test model. All dimensions are in inches.

Figure 2. - Wing-fuselage configuration.



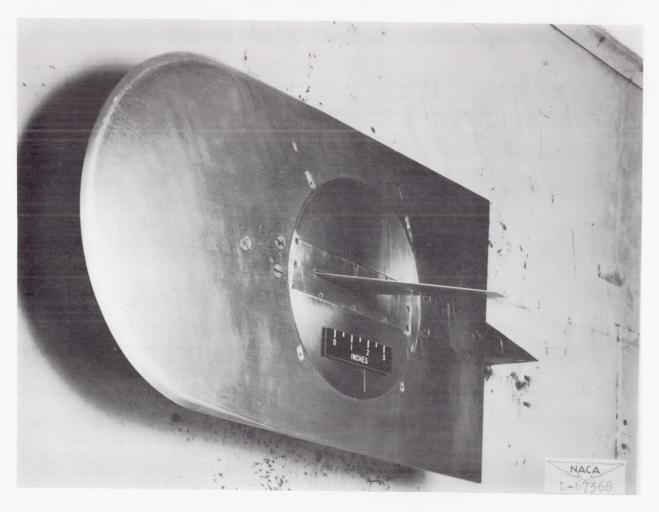
(b) Test model mounted on the sting support in the Langley high-speed $\,$ 7- by 10-foot tunnel.

Figure 2. - Concluded.



(a) Geometric characteristics of test model. All dimensions are in inches.

Figure 3. - Semispan configuration.



(b) Test model mounted on the reflection plane plate in the Langley high-speed 7- by 10-foot tunnel.

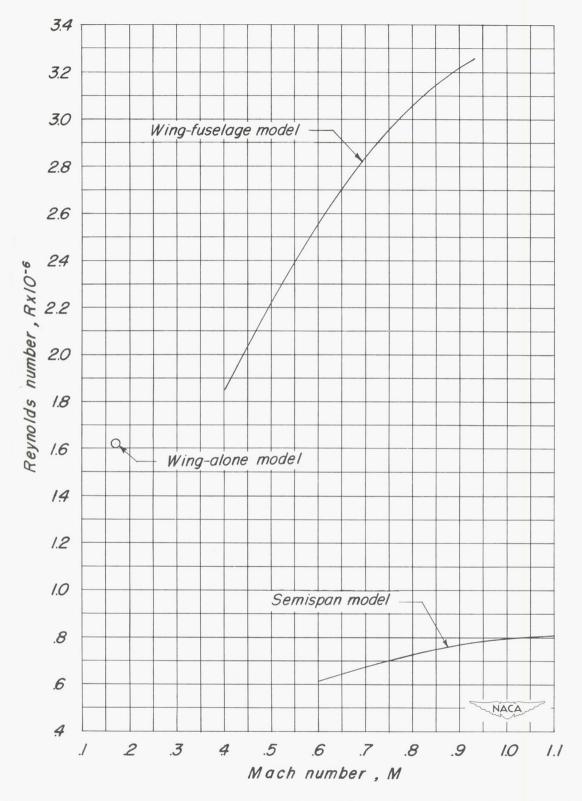
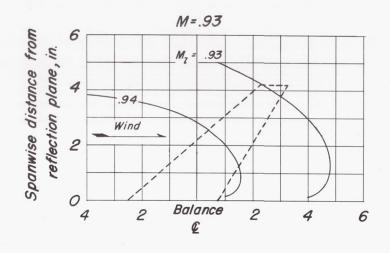
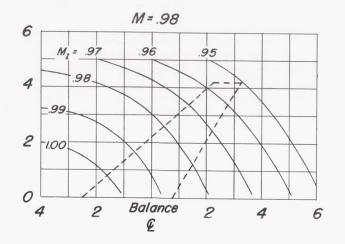
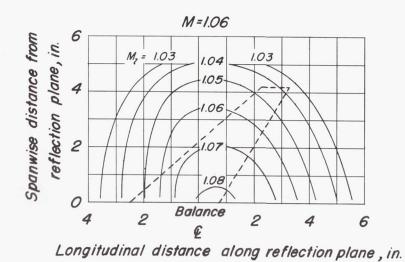


Figure 4. - Variation of mean test Reynolds number with Mach number for the various model configurations.







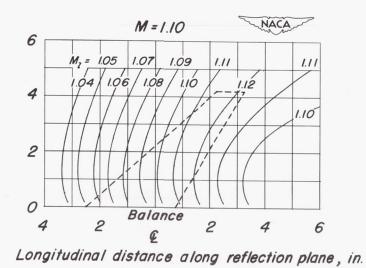
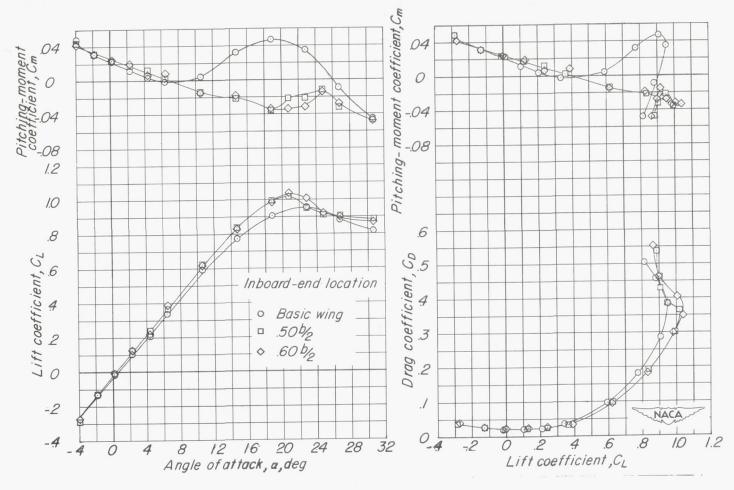


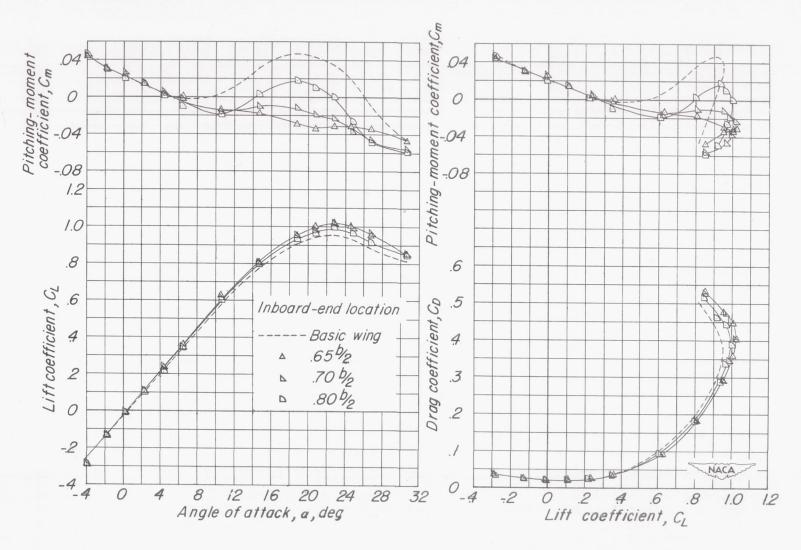
Figure 5. - Typical Mach number contours over the side-wall reflection-

plane plate in the vicinity of the semispan model.



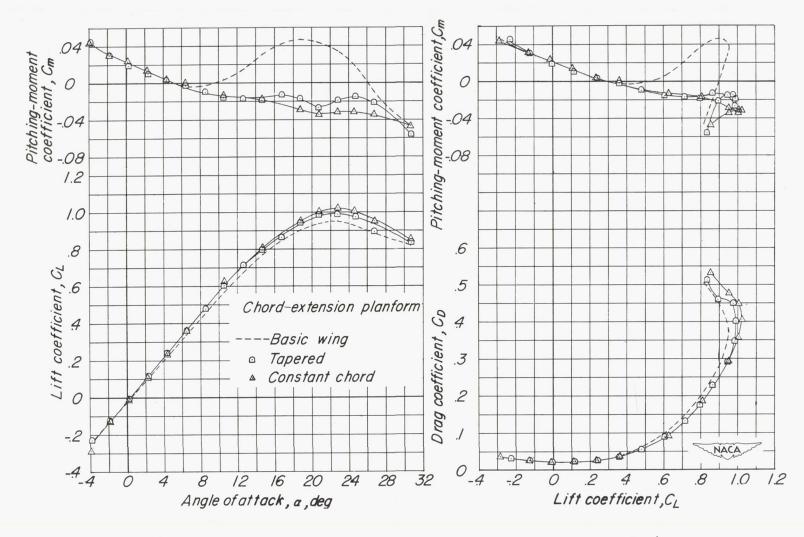
(a) Effect of inboard-end location of chord-extension.

Figure 6.- Effects of chord-extensions on the low-speed aerodynamic characteristics of the wing alone. Chord-extension extends to wing tip; chord-extension, $0.10\overline{c}$; M = 0.17.



(a) Concluded.

Figure 6.- Continued.



(b) Effect of chord-extension plan forms; inboard end at 0.65b/2.

Figure 6. - Concluded.

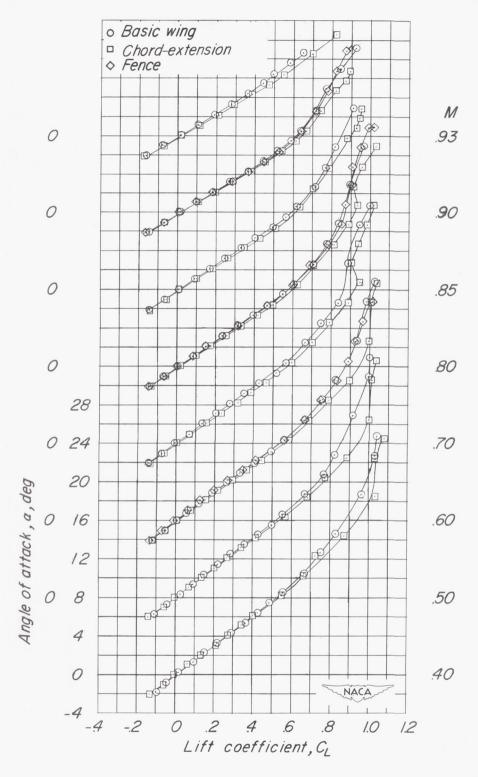


Figure 7.- Effects of chord-extensions and a wing fence on the aerodynamic characteristics of the wing-fuselage model. Chord-extension of $0.10\overline{c}$ with inboard-end location at 0.65b/2. Fence location, 0.65b/2.

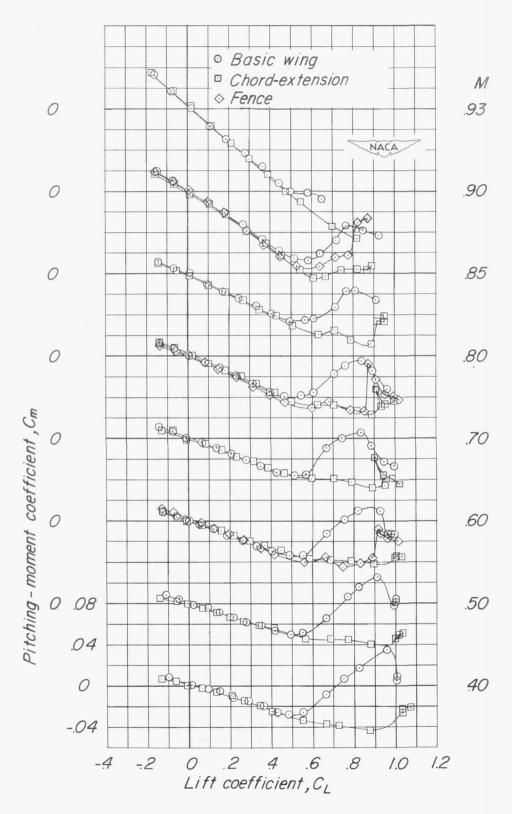


Figure 7. - Continued.

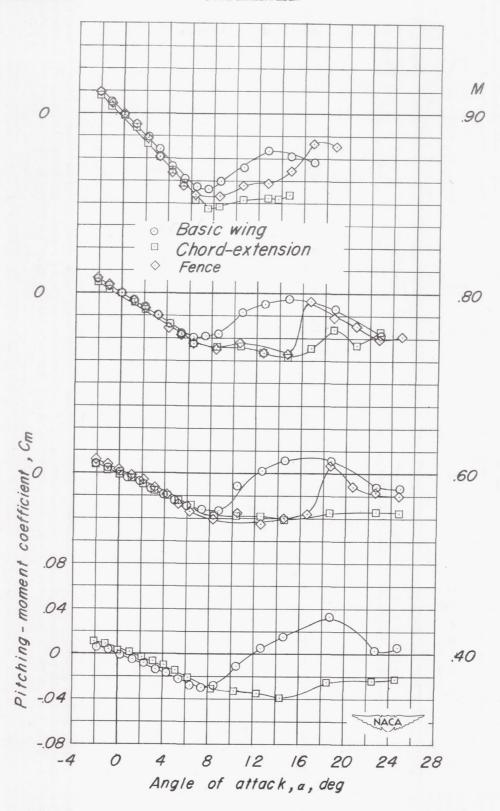


Figure 7. - Continued.

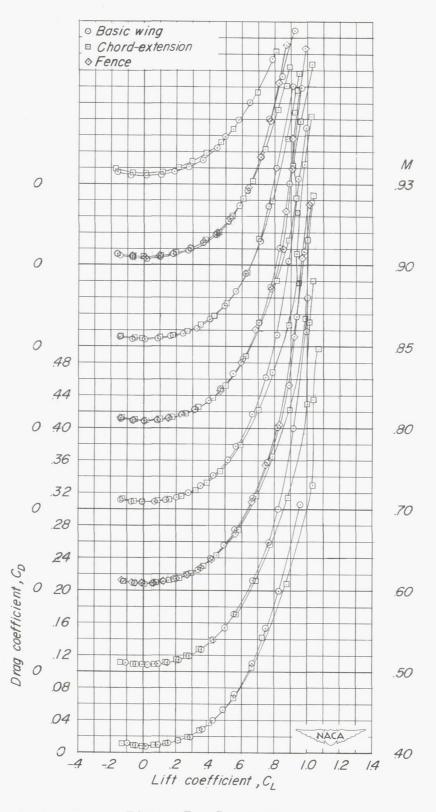


Figure 7. - Concluded.

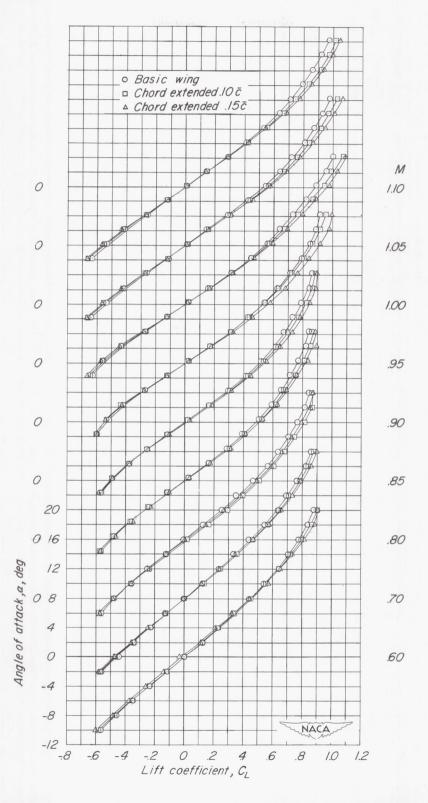


Figure 8. - Effects of chord-extensions on the aerodynamic characteristics of the semispan model. Chord-extension inboard-end location at 0.65b/2.

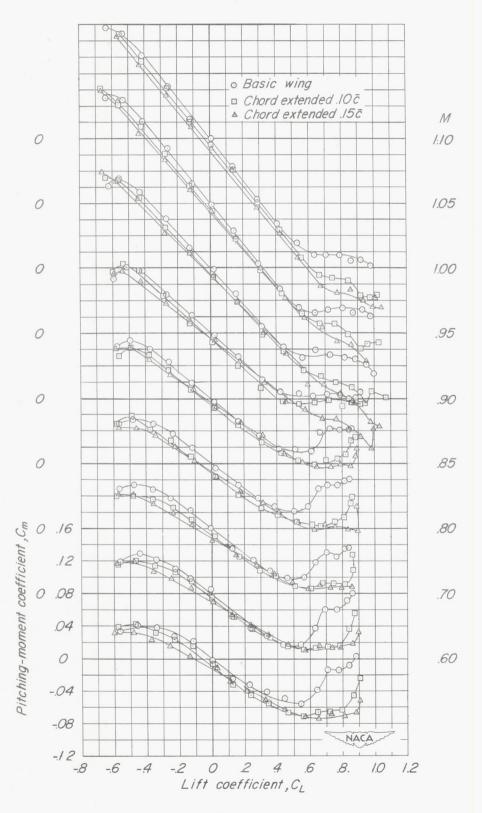


Figure 8. - Continued.

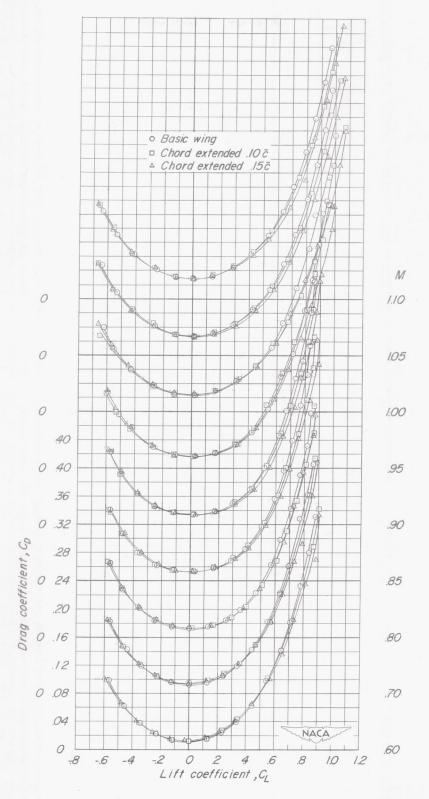


Figure 8. - Continued.

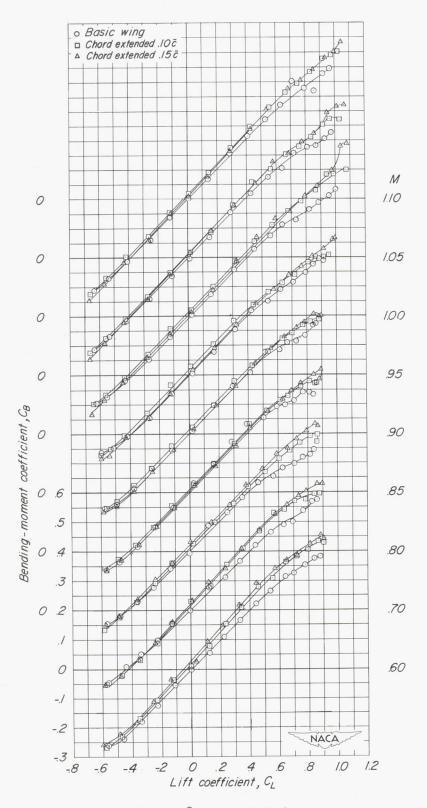
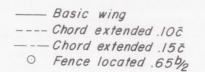
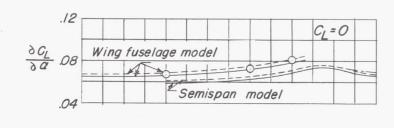
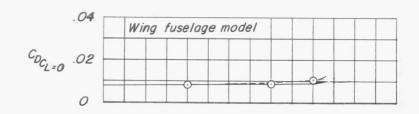
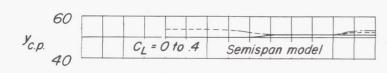


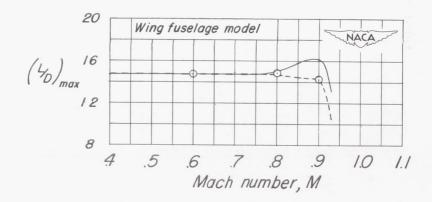
Figure 8. - Concluded.











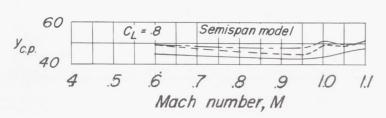
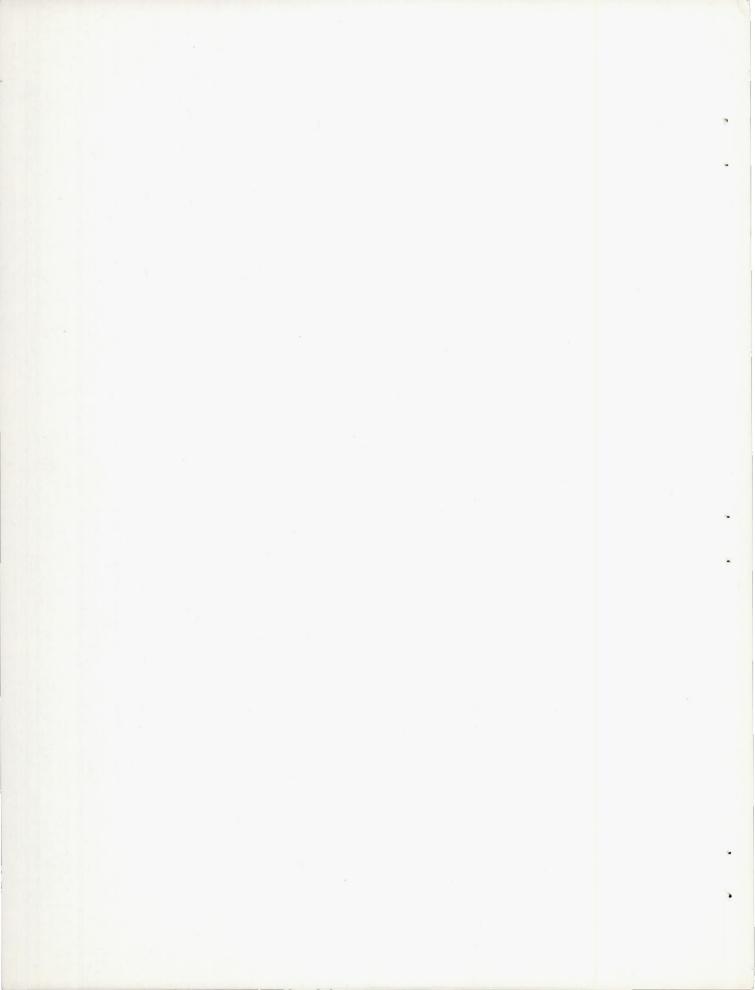
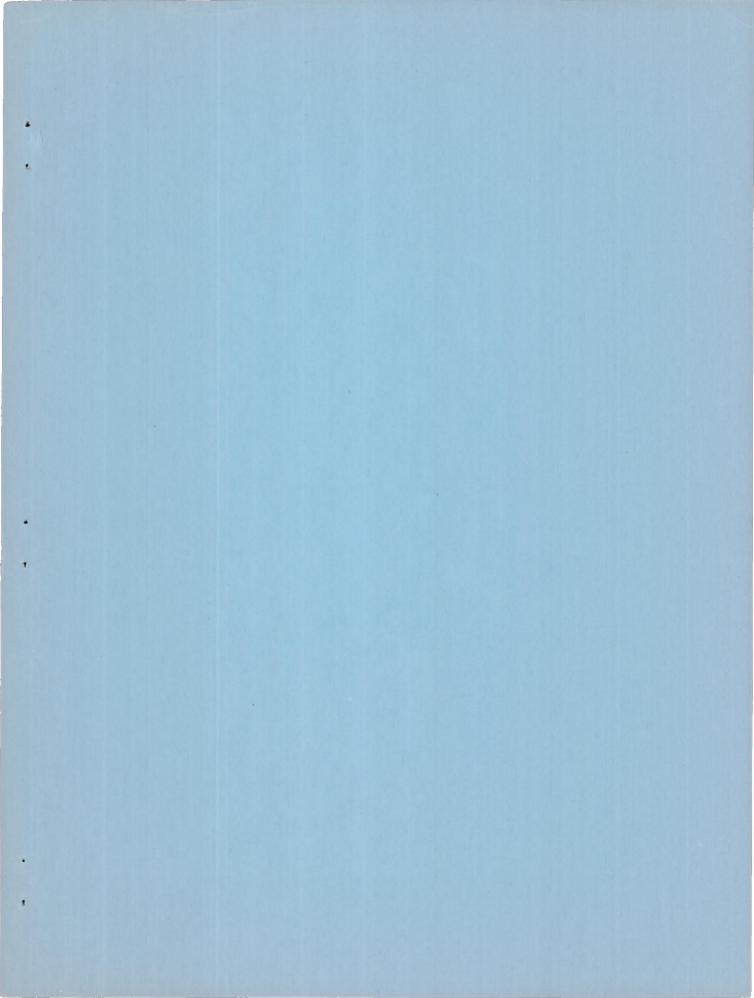


Figure 9.- Summary of aerodynamic characteristics. Chord-extension inboard-end location, 0.65b/2.





SECURITY INFORMATION CONFIDENTIAL